Synthesis, Spectroscopic Characterization, and DFT Study of (E)-N-((1-(4-fluorophenyl)-^{1}H-pyrazol-4-yl) methylene)-2-(1H-indol-3-yl) ethanimine

Kamal Raj Sapkota [1*], Vaishali Anand [2, 3], and H. C. Rai [4]
[1]Department of Chemistry, Tribhuvan University, Prithvi Narayan Campus, Pokhara, Nepal
[2]PG Department of Chemistry, Magadh University, Bodh-Gaya, Bihar, India
[3]Department of Chemistry, BRM College, Munger, Bihar, India
[4]University Department of Chemistry, BRA Bihar University, Muzaffarpur, Bihar, India
[*]**Email-**sapkotakamal69@gmail.com (KRS) and vaishaligaya150@gmail.com (VA)
https://doi.org10.3126/kanyaj.v6io1.87723

Abstract

A new Schiff base compound, **(E)-N-((1-(4-fluorophenyl)-^{1}H-pyrazol-4-yl)methylene)-2-(1H-indol-3-yl)ethanimine** (FME), was created by reacting 1-(4-fluorophenyl)-1H-pyrazole-4-carbaldehyde with 2-(1H-indol-3-yl)ethan-1-amine under condensation conditions. The molecular structure was verified using elemental analysis and a suite of spectroscopic tools, including NMR, FT-IR, UV-Vis, and mass spectrometry. Both ^1H and ^13C NMR spectra confirmed the presence of the imine bond and aromatic rings, while FT-IR and UV-Vis spectra highlighted the formation of the Schiff base and extensive π-conjugation. The mass spectrum showed a molecular ion peak at m/z 332.14, consistent with the predicted molecular weight. Frontier Molecular Orbital (FMO) analysis revealed a HOMO–LUMO energy gap of 3.951 eV, indicating stable electronic properties and potential for charge transfer. Together, these analyses confirm that FME was successfully synthesized and structurally intact, supporting its potential for exploration in materials science and biological studies.

Keywords: Carbaldehyde; Schiff's conjugate; Ethanamine, Imine, Orbital

Introduction

Research on heteroatom-containing aromatic systems has repeatedly demonstrated their importance in the creation of biologically relevant molecules, particularly those derived from pyrazole and indole units, which exhibit high adaptability within chemical and biological environments (Rohilla et al., 2024; Li, 2013; Nguyen et al., 2025). Pyrazole-based frameworks are well documented for their involvement in compounds that modulate inflammatory processes, suppress microbial growth, interfere with cancer cell proliferation, and influence metabolic pathways related to glucose regulation (Aziz et al., 2020; Alam et al., 2022; Sapkota, 2025). In a complementary manner, indole-containing structures dominate many classes of natural metabolites and pharmaceuticals, highlighting their exceptional compatibility with biological macromolecules and signaling systems (Dhiman et al., 2022; Zhang et al., 2022). Modern molecular design no longer treats such heterocycles

as isolated building blocks. Instead, emphasis is placed on constructing single molecules that incorporate multiple validated pharmacophores. The deliberate assembly of pyrazole and indole motifs within one scaffold has been shown to reshape electronic communication across the molecule, enhance interaction efficiency with biological targets, and generate compounds with improved functional characteristics when compared with individual heterocyclic units (Kabir et al., 2022; Li et al., 2021). From a synthetic standpoint, condensation-based imine formation offers a reliable pathway for producing these hybrid structures. Schiff bases generated from pyrazole-functionalized carbonyl compounds and indole-derived amines are particularly attractive, as the resulting imine linkage acts as a conduit for electronic delocalization, increases molecular rigidity, and introduces coordination behavior that is often associated with both chemical stability and biological versatility (Patel et al., 2024; Liu et al., 2020; Khan et al., 2024). In addition to scaffold hybridization, molecular performance can be further refined through strategic halogen substitution. The presence of a fluorinated aromatic moiety, especially a para-fluorophenyl group, alters electron density distribution and lipophilic balance while exerting minimal steric influence (Henary et al., 2024; Rohilla et al., 2024). These subtle changes frequently translate into enhanced resistance to metabolic breakdown, improved membrane transport, and stronger noncovalent interactions, features that are highly valued in pharmaceutical development and functional material science (Shabir et al., 2023). On the basis of these design considerations, the present study focuses on the synthesis and in-depth characterization of a newly constructed Schiff base, (E)-N-((1-(4-fluorophenyl)-1H-pyrazol-4-yl)methylene)-2-(1H-indol-3-yl)ethanamine. The compound was obtained via a mild condensation protocol and its identity was confirmed using FT-IR, NMR, and UV–visible spectroscopy. To provide a deeper understanding of its electronic features, density functional theory calculations were applied. Frontier molecular orbital analysis and molecular electrostatic potential mapping were used to assess charge distribution and identify reactive regions. The strong agreement between computational outputs and experimental observations supports the proposed structure and clarifies its electronic behavior. In conclusion, this investigation introduces a new fluorinated pyrazole–indole Schiff base and delivers a comprehensive assessment of its structural and electronic attributes. The outcomes contribute to ongoing efforts aimed at expanding heterocyclic hybrid chemistry and establish a platform for future exploration of functional and biological applications.

Research Methodology

The synthesis of (E)-N-((1-(4-fluorophenyl)-1H-pyrazol-4-yl)methylene)-2-(1H-indol-3-yl)ethanimine (FME) was carried out using chemicals procured from Sigma-Aldrich, which were used directly without any further purification.

The functional groups and vibrational modes of (E)-N-((1-(4-fluorophenyl)-1H-pyrazol-4-yl)methylene)-2-(1H-indol-3-yl)ethanimine (FME) were identified using FT-IR spectroscopy, recorded at 25 °C on a Perkin-Elmer FT-IR spectrometer. Structural characterization of the carbon and hydrogen framework was performed through ^{13}C and ^{1}H

NMR spectroscopy using a Bruker AVANCE-III spectrometer. The electronic absorption behavior of FME was explored via UV-Vis spectroscopy on a Perkin-Elmer Lambda 35 spectrometer, covering the 200–600 nm range with a 1 nm bandwidth. The mass spectrometric study was performed using a WATERS Q-ToF Premier Mass Spectrometer with electrospray ionization (ESI-MS), enabling the determination of the molecular ion peak and fragmentation pattern. Furthermore, the elemental composition of the compound was verified with a Perkin-Elmer 2400 Series II CHNS/O Analyzer, confirming its agreement with theoretical values.

Synthesis of (E)-N-((1-(4-fluorophenyl)-1H-pyrazol-4-yl)methylene)-2-(1H-indol-3-yl)ethanimine (FME)

FME was synthesized through a condensation reaction between 1-(4-fluorophenyl)-1H-pyrazole-4-carbaldehyde (1) and 2-(1H-indol-3-yl)ethan-1-amine (2), as outlined in Scheme 1. For this process, 0.50 g (3.12 mmol) of 2-(1H-indol-3-yl)ethan-1-amine (2) was dissolved in 20 mL of methanol under continuous stirring. To the resulting solution, 0.59 g (3.10 mmol) of 1-(4-fluorophenyl)-1H-pyrazole-4-carbaldehyde (1) was gradually introduced. The mixture was then heated under reflux for 5 hours, during which time a pale yellow solid began to separate as the solvent volume slowly decreased to approximately 10 mL. Upon cooling, the precipitated product was collected by filtration, rinsed successively with 5 mL of chilled methanol and 10 mL of hexane, and air-dried. The crude material was further purified via recrystallization using methanol, followed by drying under vacuum. The final product, FME, was isolated as a yellow solid with an 88% yield, amounting to 0.96 g. Theoretical investigations were carried out using Gaussian 09 (Frisch et al., 2010) in combination with GaussView (Dennington et al., 2007) software. The calculations were performed within the framework of density functional theory (DFT), applying the B3LYP functional along with the 6-311G(d,p) basis set (Jamal et al., 2024; Jamal et al., 2025).

Results and Discussion

Elemental Analysis of (E)-N-((1-(4-fluorophenyl)-1H-pyrazol-4-yl)methylene)-2-(1H-indol-3-yl)ethanamine (FME), with the chemical formula C20H17FN4, was conducted to verify its molecular composition. The observed elemental percentages were as follows: carbon (C) 72.17%, hydrogen (H) 5.06%, fluorine (F) 5.61%, and nitrogen (N) 16.72%. These experimental outcomes have been compared to the theoretical values, which were calculated as: carbon (C) 72.27%, hydrogen (H) 5.16%, fluorine (F) 5.72%, and nitrogen (N) 16.86%. The slight variations between the experimental and calculated values indicate the high accuracy of the synthesized compound. However, the structure of FME is illustrated in Figure 1.

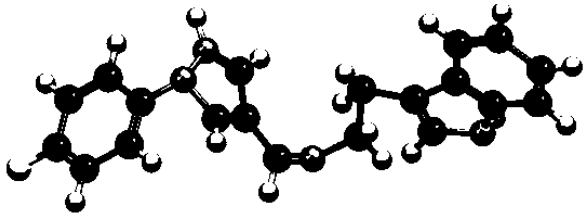

Figure 1 structure of FME

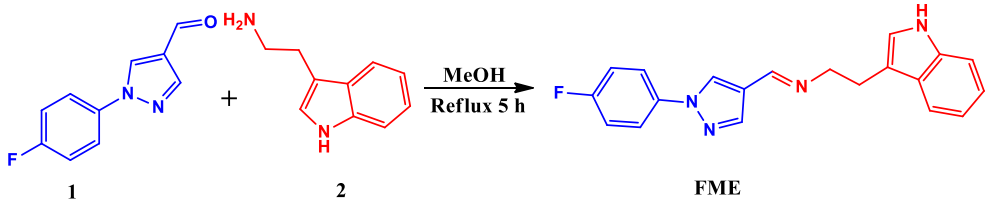

Scheme 1

NMR: The ^1H NMR spectrum (Figure 2) of **(E)-N-((1-(4-fluorophenyl)-1H-pyrazol-4-yl)methylene)-2-(1H-indol-3-yl)ethanimine (FME)**, recorded at 400 MHz in DMSO-d_6, provides valuable information about the proton environments in the molecule. A singlet observed at δ 10.00 ppm is assigned to the imine proton (–CH=N, H1), confirming the formation of the Schiff base linkage (Pavia et al., 2015; Pretsch et al., 2000). The aromatic region between δ 9.00–8.00 ppm consists of multiplets corresponding to the protons of the pyrazole and indole rings (H2–H6) (Pavia et al., 2015; Pretsch et al., 2013; Pouchert et al., 1993). Additional aromatic proton signals appear in the range δ 8.00–7.00 ppm and are attributed to the fluorophenyl ring (H7–H10). In the aliphatic region, the methylene protons adjacent to the indole ring (H11) resonate as a singlet at δ 3.00–2.00 ppm, while the methylene protons of the ethanamine side chain (H12) appear between δ 2.00–1.00 ppm (Pavia et al., 2015; Pretsch et al., 2000; Pretsch et al., 2013; Sharma, 2007; Stothers, 2012; Pouchert et al., 1993). Overall, the ^1H NMR data confirm the presence of all expected proton environments in FME.

The ^13C NMR spectrum (Figure 2), recorded at 100 MHz in DMSO-d_6, further supports the proposed structure. **For clarity, the carbon numbering used in the discussion is illustrated in the adjacent molecular structure (Figure 3).** A distinct downfield signal at δ ~160 ppm is assigned to the imine carbon (C1, C=N), reflecting its deshielded nature, while the fluorine-substituted quaternary carbon of the phenyl ring (C7) also contributes to this region due to the strong electronegative effect of fluorine (Pavia et al., 2015; Sharma, 2007). A resonance observed at δ ~140 ppm corresponds to a quaternary carbon of the pyrazole ring (C3). Multiple signals appearing in the δ 140–120 ppm region are attributed to aromatic carbons of the pyrazole (C2, C4), fluorophenyl (C5–C9), and indole rings (C10–C14). Additional aromatic carbons from the indole system resonate in the δ 120–110 ppm range (C15–C17) (Pavia et al., 2015; Sharma, 2007; Pouchert et al., 1993). The methylene carbon linking the indole moiety to the ethanamine chain (C18) appears between δ 60–70 ppm, while the terminal methylene carbon of the ethanamine side

chain (C19) is observed in the δ 30–20 ppm region (Pavia et al., 2015; Sharma, 2007; Stothers, 2012; Pouchert et al., 1993). The close correspondence between the experimental ^13C NMR chemical shifts and the numbered carbon centers shown in Figure 3 strongly confirms the structural integrity of FME.

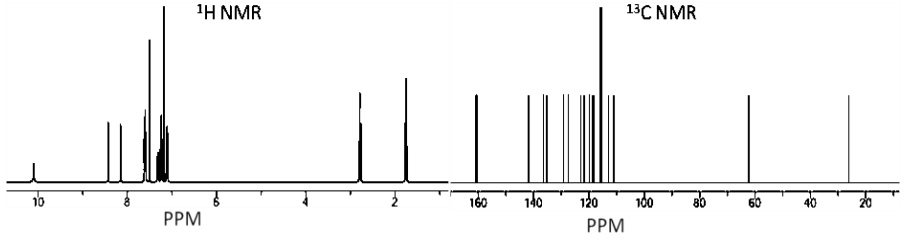

Figure 2 NMR for FME

FT-IR Spectral Analysis: The functional groups present in (E)-N-((1-(4-fluorophenyl)-1H-pyrazol-4-yl)methylene)-2-(1H-indol-3-yl)ethanamine (FME) were confirmed by FT-IR spectrum (Figure 3). The infrared spectrum was recorded using KBr pellets, and the characteristic absorption peaks were observed at specific wavenumbers (cm^{-1}), in agreement with the proposed structure. A broad and strong absorption at 3500 cm^{-1} is attributed to the N–H stretching vibration, confirming the presence of both the indole and amine functionalities (Pavia et al., 2015; Socrates, 2004). The absorption band at 3059 cm^{-1} corresponds to aromatic C–H stretching vibrations, indicating the presence of multiple aromatic rings in the molecular framework (Sharma, 2007; Socrates, 2004). A sharp and intense peak at 1684 cm^{-1} is characteristic of the imine (C=N) stretching, providing evidence for the Schiff base linkage formation between the pyrazole moiety and the indole derivative. Bands at 1643 and 1614 cm^{-1} are assigned to C=C stretching vibrations of the aromatic systems, including both the indole ring and the pyrazole fragment, while the peak at 1582 cm^{-1} is further associated with conjugated C=C stretching within the aromatic and heterocyclic environment (Pavia et al., 2015; Pretsch et al., 2000; Socrates, 2004). Additional peaks at 1446 cm^{-1} and 1399 cm^{-1} are due to C–C stretching and C–N stretching vibrations, respectively, which support the presence of aromatic and heterocyclic structures (Pavia et al., 2015; Pretsch et al., 2013; Socrates, 2004). The band at 1333 cm^{-1} is assigned to C–N stretching, which is particularly significant for confirming the presence of the pyrazole core. The absorption at 1218 cm^{-1} is characteristic of the C–F stretching vibration, confirming the substitution of the fluorine atom on the phenyl ring (Pavia et al., 2015; Sharma, 2007; Socrates, 2004).

Further absorptions at 1177 cm^{-1} and 1070 cm^{-1} correspond to C–N stretching and C–H in-plane bending vibrations, respectively. Bands at 1009 and 957 cm^{-1} are attributed to aromatic C–H bending modes (Pretsch et al., 2000; Sharma, 2007; Stothers, 2012; Socrates, 2004). The out-of-plane C–H bending vibrations of substituted aromatic systems appear at 828, 755, and 731 cm^{-1}. The lower wavenumber region shows peaks at 658, 573, and 516 cm^{-1}, which are assigned to skeletal vibrations involving the aromatic framework

and heterocyclic rings (Pavia et al., 2015; Stothers, 2012; Socrates, 2004). Overall, the FT-IR data confirm the successful formation of the target Schiff base derivative FME.

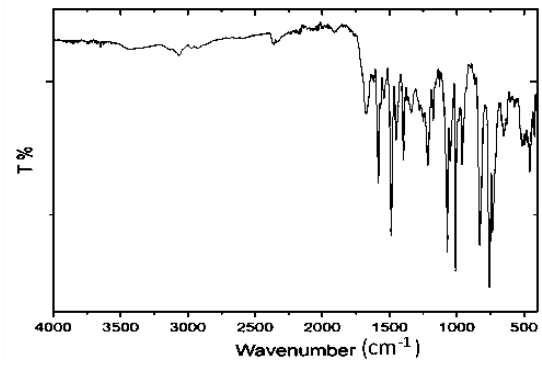

Figure 3 FT-IR for FME

UV-Visible Spectral Analysis: The electronic absorption behavior of **(E)-N-((1-(4-fluorophenyl)-1H-pyrazol-4-yl)methylene)-2-(1H-indol-3-yl)ethanimine (FME)** was examined using UV–Visible spectroscopy (Figure 4) in order to assess the influence of its molecular architecture on electronic transitions. The recorded spectrum shows two absorption features, each originating from different electronic processes within the molecule. A dominant absorption maximum is observed at 318 nm, which can be associated with a $\pi \rightarrow \pi^*$ excitation (Pavia et al., 2015; Sharma, 2007). The appearance of this band at a relatively longer wavelength reflects the presence of an efficient electron-delocalization pathway throughout the molecule. This effect arises from the structural connection between the indole fragment, the azomethine (C=N) bridge, and the pyrazole ring, which together facilitate communication between π systems. As a result, the energy required for electronic excitation is reduced, allowing absorption to occur at lower energies (Pavia et al., 2015; Pretsch et al., 2000; Pretsch et al., 2013; Sharma, 2007). Alongside this intense band, a weaker absorption is detected at 275 nm. This transition is attributed to $\pi \rightarrow \pi^*$ excitations that remain largely confined within individual aromatic subunits of the molecule, particularly the indole and pyrazole rings. Since these transitions do not involve the full conjugated framework, they require higher excitation energy and therefore appear at shorter wavelengths (Pavia et al., 2015; Sharma, 2007; Pretsch et al., 2013). Overall, the UV–Visible absorption pattern confirms that FME behaves as a conjugated system in which the azomethine linkage plays a central role in extending π-electron delocalization across heteroaromatic units. The observed spectral features are consistent with those commonly reported for Schiff base compounds incorporating aromatic and heterocyclic components, supporting the proposed electronic structure of the molecule.

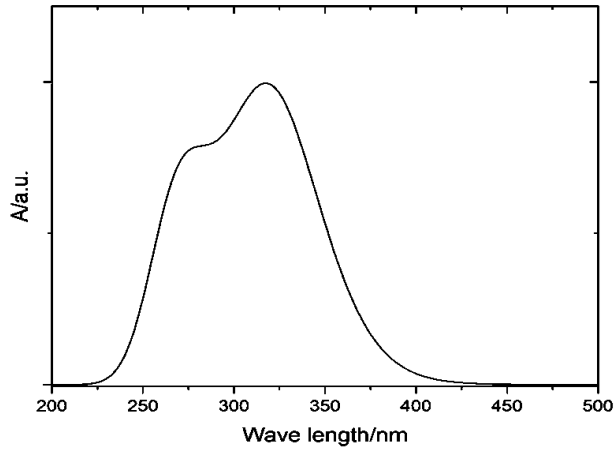

Figure 4 UV-Vis for FME

Frontier Molecular Orbital (FMO) Analysis: The electronic behavior of **(E)-N-((1-(4-fluorophenyl)-1H-pyrazol-4-yl)methylene)-2-(1H-indol-3-yl)ethanimine (FME)** was evaluated through frontier molecular orbital calculations in order to understand how electron distribution influences stability and reactivity. The calculated HOMO energy is −5.489 eV, while the LUMO is positioned at −1.538 eV, resulting in an energy separation of 3.951 eV. This magnitude of energy gap suggests that the molecule maintains sufficient electronic stability while still allowing electronic excitation and redistribution under suitable conditions (Jamal et al., 2024; Jamal et al., 2025; Yu et al., 2022; Islam et al., 2024). Visualization of the frontier orbitals (Figure 5) reveals a clear division of electron density across different molecular fragments. The HOMO is largely concentrated on the indole-containing 2-(1H-indol-3-yl)ethan-1-amine segment. Owing to the electron-rich character of the indole nucleus, this region is expected to act as the primary source of electron donation during molecular interactions, including those relevant to biological recognition processes (Jamal et al., 2025; Yu et al., 2022; Islam et al., 2024). In contrast, the LUMO is mainly distributed over the pyrazole ring and the attached fluorophenyl group, forming an electron-deficient zone within the molecule. This localization indicates that this portion of FME is more favorable for accepting electron density and may serve as the principal interaction site during charge-transfer processes or noncovalent binding events such as π–π interactions and hydrogen bonding (Jamal et al., 2024; Jamal et al., 2025). The calculated HOMO–LUMO separation reflects a balance between rigidity and electronic adaptability, a feature commonly observed in molecules suitable for optoelectronic applications and molecular recognition systems. Moreover, the spatial separation between donor-rich and acceptor-rich regions supports the possibility of intramolecular charge transfer upon excitation, which is often associated with enhanced nonlinear optical responses and favorable bioactive behavior (Jamal et al., 2024; Jamal et al., 2025; Yu et al., 2022; Islam et al., 2024; Jayasundara, 2019). Overall, the FMO results demonstrate that the combined presence of indole, pyrazole, and fluorophenyl fragments plays a decisive role in shaping the electronic architecture of FME. These insights are valuable for guiding future structure–

activity relationship studies and for designing related molecules with tailored electronic properties.

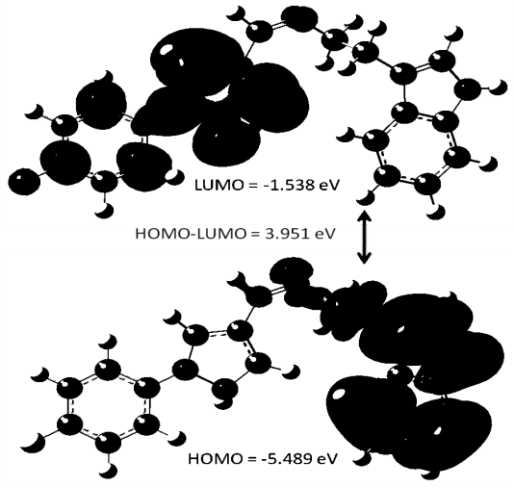

Figure 5 FMO for FME

Conclusion

In this study, the Schiff base derivative (E)-N-((1-(4-fluorophenyl)-1H-pyrazol-4-yl)methylene)-2-(1H-indol-3-yl)ethanamine (FME) was successfully synthesized through a simple condensation reaction and thoroughly characterized using elemental analysis, NMR, FT-IR, UV-Vis, and mass spectrometry. The spectral data fully support the proposed structure, confirming the formation of the imine linkage and the presence of fluorinated and indole-based aromatic systems. The mass spectrum verified the molecular ion peak, and the observed UV-Vis absorption bands highlight the extended π-conjugation within the molecule. Additionally, frontier molecular orbital analysis revealed a moderate HOMO-LUMO energy gap, suggesting favorable electronic stability and potential reactivity. Overall, the structural and theoretical studies validate the successful design and synthesis of FME, exhibiting its potential as an advantageous candidate for future uses in material science, optoelectronics, and medicinal chemistry.

Declaration of Competing Interest

None

References

Alam, M. J., Alam, O., Naim, M. J., Nawaz, F., Manaithiya, A., Imran, M., ... & Shakeel, F. (2022). Recent advancement in drug design and discovery of pyrazole biomolecules as cancer and inflammation therapeutics. Molecules, 27(24), 8708.

Aziz, H., Zahoor, A. F., & Ahmad, S. (2020). Pyrazole bearing molecules as bioactive scaffolds: A review. Journal of the Chilean Chemical Society, 65(1), 4746-4753.

Dennington, R. D. II, Keith, T., & Millam, J. (2007). GaussView (Version 4.1.2). Semichem Inc.

Dhiman, A., Sharma, R., & Singh, R. K. (2022). Target-based anticancer indole derivatives and insight into structure–activity relationship: A mechanistic review update (2018–2021). Acta Pharmaceutica Sinica B, 12(7), 3006-3027.

Frisch, M. J., Trucks, G. W., Schlegel, H. B., Scuseria, G. E., Robb, M. A., Cheeseman, J. R., Scalmani, G., Barone, V., Mennucci, B., Petersson, G. A., et al. (2010). Gaussian 09 Revision E.01. Gaussian, Inc.

Henary, E., Casa, S., Dost, T. L., Sloop, J. C., & Henary, M. (2024). The role of small molecules containing fluorine atoms in medicine and imaging applications. Pharmaceuticals, 17(3), 281.

Islam, S., Mansha, A., & Asim, S. (2024). Effects of Metal Ions and Substituents on HOMO–LUMO Gap Evident from UV–Visible and Fluorescence Spectra of Anthracene Derivatives. Journal of Fluorescence, 34(6), 2495-2512.

Jamal, A., & Faizi, M. S. H. (2024). Synthesis, structural characterization, DFT calculations, and molecular docking of a novel quinoline derivative. Journal of Molecular Structure, 1300, 137251.

Jamal, A., Faizi, M. S. H., & Ferjani, H. (2025). Designing of quinoline-based esterase inhibitor: Synthesis, crystal structure, DFT calculations, and molecular docking. Journal of Molecular Structure, 1319, 139540.

Jamal, A., Faizi, M. S. H., & Roy, A. K. (2025). Synthesis, Crystal Structure, and Spectroscopic Study of a Novel Quinoline Derivative with Nonlinear Optical Activity and Esterase Inhibition Potential. Journal of Molecular Structure, 144407.

Jayasundara, S. (2019). Computational investigation of the tunability of HOMO-LUMO levels and band gaps in conducting polymers.

Kabir, A., & Muth, A. (2022). Polypharmacology: The science of multi-targeting molecules. Pharmacological Research, 176, 106055.

Khan, Z., & Tanoli, M. A. K. (2024). Exploring The Legacy: The Biological Interactions of Bis Schiff Bases and Their Coordinated Azomethine Derivatives Over Time. Pakistan Journal of Medicine and Dentistry, 13(2), 90-101.

Li, J. J. (Ed.). (2013). Heterocyclic chemistry in drug discovery. John Wiley & Sons.

Li, X., Li, X., Liu, F., Li, S., & Shi, D. (2021). Rational multitargeted drug design strategy from the perspective of a medicinal chemist. Journal of Medicinal Chemistry, 64(15), 10581-10605.

Liu, H., Chu, Z. W., Xia, D. G., Cao, H. Q., & Lv, X. H. (2020). Discovery of novel multi-substituted benzo-indole pyrazole schiff base derivatives with antibacterial activity targeting DNA gyrase. Bioorganic Chemistry, 99, 103807.

Nguyen, H. T., Doan, V. T. C., Nguyen, T. H., & Tran, M. H. (2025). Recent advances in metal-free catalysts for the synthesis of N-heterocyclic frameworks focusing on 5- and 6-membered rings: a review. RSC Advances, 15(13), 9676-9755.

Patel, G., Shah, V. R., Nguyen, T. A., & Deshmukh, K. (Eds.). (2024). Spirooxindole: Chemistry, synthesis, characterization and biological significance. Elsevier.

Pavia, D. L., Lampman, G. M., Kriz, G. S., & Vyvyan, J. R. (2015). Introduction to spectroscopy.

Pouchert, C. J., & Behnke, J. (1993). The Aldrich library of ^{13}C and ^{1}H FT NMR spectra. Aldrich Chemical Co, 1085.

Pretsch, E., Bühlmann, P., & Affolter, C. (2000). Structure determination of organic compounds. Springer-Verlag.

Pretsch, E., Clerc, T., Seibl, J., & Simon, W. (2013). Tables of spectral data for structure determination of organic compounds. Springer Science & Business Media.

Ríos-Gutiérrez, M., Saz Sousa, A., & Domingo, L. R. (2023). Electrophilicity and nucleophilicity scales at different DFT computational levels. Journal of Physical Organic Chemistry, 36(7), e4503.

Rohilla, S., Goyal, G., Berwal, P., & Mathur, N. (2024). A Review on Indole-triazole Molecular Hybrids as a Leading Edge in Drug Discovery: Current Landscape and Future Perspectives. Current Topics in Medicinal Chemistry, 24(18), 1557-1588.

Sapkota, K. R. (2025). Synthesis, Characterization, and Structural Elucidation of a Novel (E)-1-(1-Phenyl-1H-pyrazol-4-yl)-N-(1-(p-tolyl)-1H-pyrazol-5-yl) methanimine. INTELLIGENCE Journal of Multidisciplinary Research, 4(1), 67-80.

Shabir, G., Saeed, A., Zahid, W., Naseer, F., Riaz, Z., Khalil, N., ... & Albericio, F. (2023). Chemistry and pharmacology of fluorinated drugs approved by the FDA (2016–2022). Pharmaceuticals, 16(8), 1162.

Sharma, Y. R. (2007). Elementary organic spectroscopy. S. Chand Publishing.

Socrates, G. (2004). Infrared and Raman characteristic group frequencies: Tables and charts. John Wiley & Sons.

Stothers, J. (2012). Carbon-13 NMR Spectroscopy: Organic Chemistry, A Series of Monographs, Volume 24 (Vol. 24). Elsevier.

Yu, J., Su, N. Q., & Yang, W. (2022). Describing chemical reactivity with frontier molecular orbitalets. JACS Au, 2(6), 1383-1394.

Zhang, H. H., & Shi, F. (2022). Organocatalytic atroposelective synthesis of indole derivatives bearing axial chirality: strategies and applications. Accounts of Chemical Research, 55(18), 2562-2580.